



Cite this: *RSC Adv.*, 2022, 12, 15728

Structure–antitumor activity relationship of hybrid acetogenins focusing on connecting groups between heterocycles and the linker moiety†

Kaito Ohta,^a Tetsuya Fushimi,^b Mutsumi Okamura,^c Akinobu Akatsuka,^c Shingo Dan,^c Hiroki Iwasaki,^a Masayuki Yamashita^a and Naoto Kojima *^a

We studied hybrid molecules of annonaceous acetogenins and mitochondrial complex I-inhibiting insecticides to develop a novel anticancer agent. A structure–antitumor activity relationship study focusing on the connecting groups between the heterocycles and the linker moiety bearing the tetrahydrofuran moiety was conducted. Eleven hybrid acetogenins with 1-methylpyrazole instead of γ -lactone were synthesized and their growth inhibitory activities against 39 human cancer cell lines were evaluated. The nitrogen atom at the 2'-position of the linker moiety was essential for inhibiting cancer growth. The 1-methylpyrazole-5-sulfonamide analog showed potent growth inhibition of NCI-H23, a human lung cancer cell line, in a xenograft mouse assay without critical toxicity. Hence, the results of this study may pave the way for the development of novel anticancer agents, with both selective and broad anticancer activities.

Received 14th April 2022
Accepted 17th May 2022
DOI: 10.1039/d2ra02399g
rsc.li/rsc-advances

Introduction

Cancer is the leading cause of mortality worldwide, accounting for approximately 10 million deaths in 2020.¹ Cancer treatment typically includes chemotherapy, radiation therapy, and/or surgery. More recently, immunotherapy has also been employed for the treatment of cancer. Unfortunately, several other types of cancers remain difficult to treat with known anticancer drugs. Therefore, the development of drugs with novel mechanisms is crucial. Recently, examination of the inhibitors of mitochondrial complex I (reduced nicotinamide-adenine dinucleotide-ubiquinone oxidoreductase) has garnered significant interest.² For example, Kawada and co-workers reported that mitochondrial complex I inhibitors selectively suppress tumor growth through concomitant acidification of the intra- and extra-cellular environment since tumor tissues comprise more stromal cells, whose energy production depends on oxidative phosphorylation in the mitochondria, rather than normal tissues.³ One such inhibitor, darinaparsin, has been submitted to regulatory authorities designated as

a treatment for relapsed or refractory peripheral T-cell lymphoma in June 2021.⁴

Owing to our interest in complex I inhibitors, we have studied the structure–activity relationship (SAR) of annonaceous acetogenins and their analogs.⁵ Annonaceous acetogenins are polyketides isolated from *Annona* plants, which show antitumor activity against human cancer cells by inhibiting mitochondrial complex I.^{6,7} Most of them have one to three tetrahydrofuran (THF) rings in the center of the long hydrocarbon chain and an α,β -unsaturated- γ -lactone ring at the end of the molecule. In contrast, mitochondrial complex I-inhibiting insecticides (*e.g.*, tebufenpyrad) typically comprise *N*-containing heterocycles with hydrophobic side chains (Fig. 1).⁸

We hypothesized that an acetogenin analog with an *N*-containing heterocycle in place of the γ -lactone ring⁹ can act as a novel antitumor agent because the structural features of acetogenins and insecticides are similar; in addition, both are known to bind to the ND1 subunit in the mitochondria.¹⁰ Solamin was selected as a mother compound because it is a mono-THF acetogenin with a simple structure; however, it comprises all characteristic components of acetogenins.¹¹ We have previously reported that a hybrid¹² analog **1** with 1-methylpyrazole showed 80-fold higher growth inhibitory activity against NCI-H23, a human lung cancer cell line, than solamin.¹³ Subsequently, the effect of the connecting group between heterocycles and hydrophobic parts bearing the THF moiety on their biological activities was examined because 1-methylpyrazole groups of most insecticides are linked to the hydrophobic sections with an amide group. Preliminary data have shown that

^aKyoto Pharmaceutical University, 1 Misasagi-Shichono-cho, Yamashina-ku, Kyoto 607-8412, Japan. E-mail: kojima@mb.kyoto-phu.ac.jp

^bGraduate School of Pharmaceutical Sciences, Osaka University, 1-6 Yamadaoka, Suita, Osaka 565-0871, Japan

^cCancer Chemotherapy Center, Japanese Foundation for Cancer Research, 3-8-1 Ariake-ku, Tokyo 135-8550, Japan

† Electronic supplementary information (ESI) available. See <https://doi.org/10.1039/d2ra02399g>



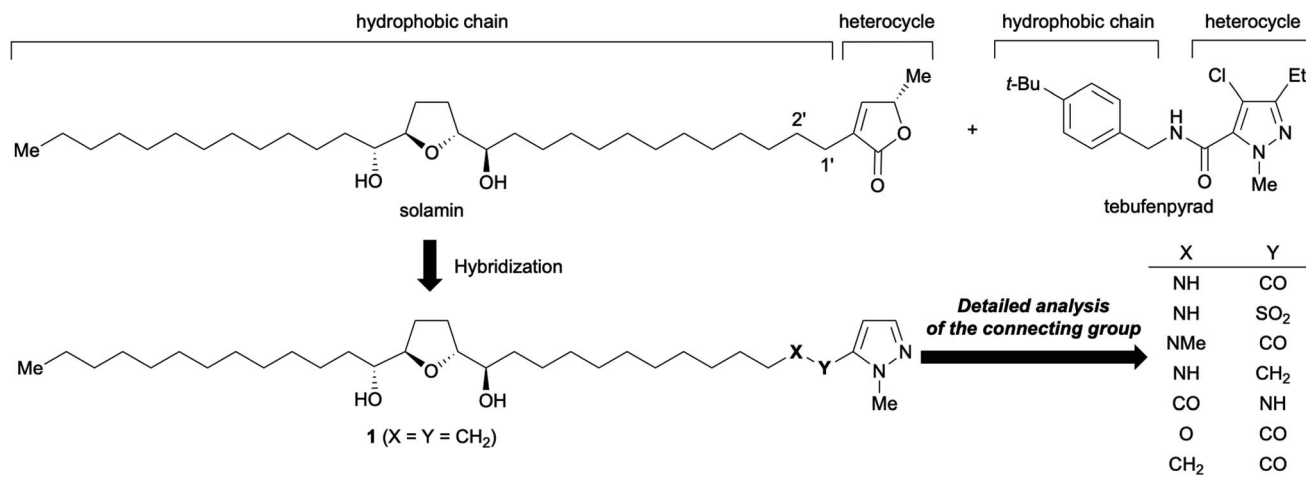


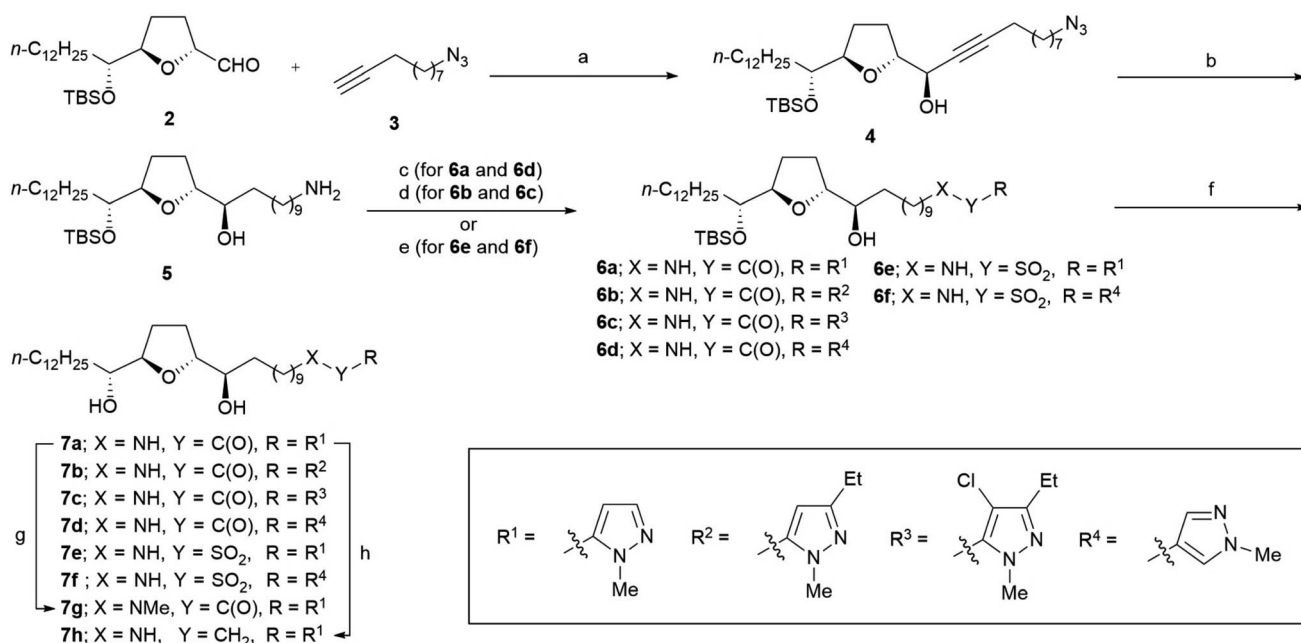
Fig. 1 Synthesis of hybrid acetogenin 1-methylpyrazole analogs.

the connecting group significantly influences the biological activity; for instance, an analog linked *via* an amide group has a potent growth inhibitory activity against some human cancer cell lines.¹⁴ This study reports (1) the synthesis of hybrid acetogenins with sulfonamide and ketomethylene bond as an amido bond's bioisosteres, (2) analysis of the effects of connecting groups on growth inhibitory activities against human cancer cell lines, (3) the effects of substituents on 1-methylpyrazole, and (4) *in vivo* mice xenograft studies.

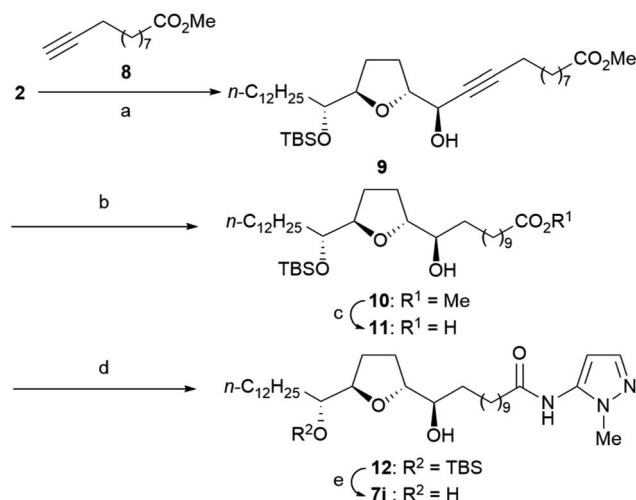
Results and discussion

Synthesis of hybrid acetogenins

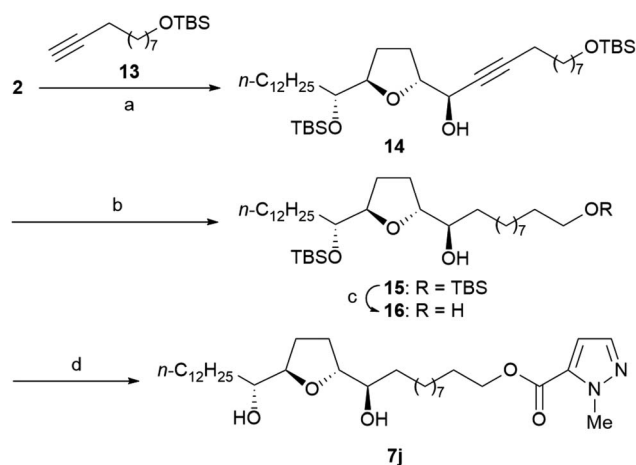
The synthesis of all analogs **7a–7k** was initiated using a common α -tetrahydrofuranyl aldehyde **2** prepared by a method previously reported by us.¹⁵ Scheme 1 illustrates the synthesis of analogs **7a–7h**. Under Carreira's conditions,¹⁶ the asymmetric alkynylation of **2** with 10-azido-1-decyne **3** resulted in a high yield of propargyl alcohol **4**, which shows a high diastereoselectivity; this *threo/trans/threo* stereochemical



Scheme 1 Synthesis of analogs **7a–7h**. Reagents and conditions: (a) Zn(OTf)₂, (1*R*,2*S*)-(–)-*N*-methylphedrine, Et₃N, toluene, rt, 84%, dr = 96 : 4; (b) H₂ (3 atm), Pd(OH)₂–C, EtOAc, rt, 79%; (c) R–COOH, EDC, DMAP, THF, rt, **6a** (85%); **6d** (51%); (d) R–COOH, DCC, DMAP, THF, rt; (e) R–SO₂Cl, Et₃N, CH₂Cl₂, rt, **6e** (73%); **6f** (73%); (f) 48% HF aq., THF/MeCN, rt, **7a** (75%); **7b** (35% from **4**); **7c** (50% from **4**); **7d** (quant.); **7e** (93%); **7f** (96%); (g) MeI, NaH, DMF, 0 °C, 60%; (h) BH₃·SMe₂, THF, reflux, 27%. DCC = *N,N'*-dicyclohexylcarbodiimide, DMAP = *N,N*-dimethylaminopyridine, EDC = 1-(3-dimethylaminopropyl)-3-ethylcarbodiimide.

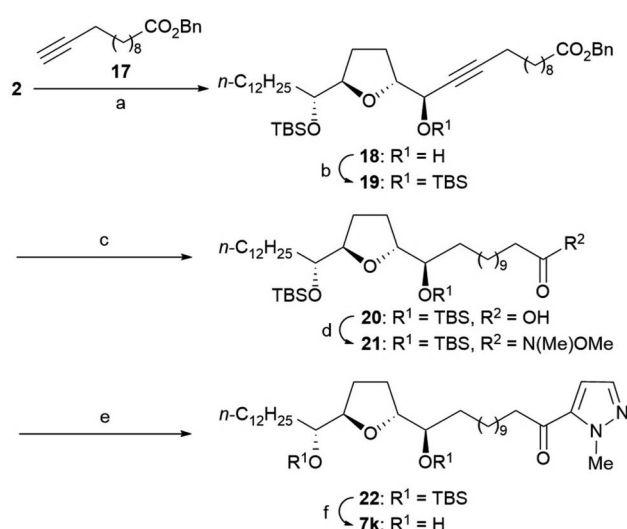


Scheme 2 Synthesis of inverse amide **7i**; reagents and conditions: (a) $\text{Zn}(\text{OTf})_2$, (1*R*,2*S*)-(–)-*N*-methylephedrine, Et_3N , toluene, rt, 77%, dr = 96 : 4; (b) H_2 (1 atm), $\text{Pd}(\text{OH})_2\text{-C}$, EtOAc , rt, 96%; (c) 1*N* NaOH, MeOH, reflux, 82%; (d) 5-amino-1-methylpyrazole, EDC, DMAP, THF, 0 °C to rt, 74%; (e) 48% HF aq., THF/MeCN, rt, 88%.



Scheme 3 Synthesis of ester **7j**; reagents and conditions: (a) $\text{Zn}(\text{OTf})_2$, (1*R*,2*S*)-(–)-*N*-methylephedrine, Et_3N , toluene, rt, 68%, dr = 95 : 5; (b) H_2 (3 atm), $\text{Pd}(\text{OH})_2\text{-C}$, EtOAc , rt, 82%; (c) 48% HF aq., THF/MeCN, rt, 84%; (d) 1-methylpyrazole-5-carboxylic acid, EDC, DMAP, THF, 0 °C to rt, 43% (67% brsm).

configuration on **4** is the same as that of the stereoisomer, which is reported to show the most potent anti-tumor activity.¹⁷ The reduction of azide and the alkyne moiety of **4** was simultaneously carried out to obtain primary amine **5**. Then, amine **5** was condensed to 1-methylpyrazole-5-carboxylic acid with 1-(3-dimethylaminopropyl)-3-ethylcarbodiimide (EDC), resulting in a good yield of amide **6a**. Substituted pyrazole-5-carboxamides **6b–6c** and pyrazole-4-carboxamide **6d** were also prepared using a similar procedure, resulting in moderate yields. The sulfonamides **6e–6f** were synthesized from **5** using the corresponding sulfonyl chlorides in the presence of Et_3N . Deprotection of *tert*-butyldimethylsilyl (TBS) ether in **6a–6f** under



Scheme 4 Synthesis of ketomethylene **7k**; reagents and conditions: (a) $\text{Zn}(\text{OTf})_2$, (1*R*,2*S*)-(–)-*N*-methylephedrine, Et_3N , toluene, rt, 73%, dr = 92 : 8; (b) TBSOTf, 2,6-lutidine, CH_2Cl_2 , rt, quant.; (c) H_2 (1 atm), 10% Pd-C, EtOAc , rt, 96%; (d) *N,O*-dimethylhydroxylamine, EDC, Et_3N , DMAP, CH_2Cl_2 , rt, 94%; (e) 5-iodo-1-methylpyrazole, *n*-BuLi, THF, –30 °C to rt, 44% (66% brsm); (f) 48% HF aq., THF/MeCN, rt, quant.

acidic conditions resulted in moderate to good yields of the desired analogs **7a–7f**. *N*-Methyl amide **7g** was synthesized by *N*-methylation of **7a** using methyl iodide under basic conditions. The reduction of **7a** using $\text{BH}_3\cdot\text{SME}_2$ in THF under reflux conditions produced amine **7h**, albeit with a low yield.

The synthesis of inverse amide **7i** was initiated *via* the same reaction as that used for the synthesis of **4** using methyl undec-10-ynoate **8** instead of **3** to obtain propargyl alcohol **9** with high diastereoselectivity (Scheme 2). Good yields of carboxylic acid **11** were obtained *via* hydrogenation of propargyl alcohol **9**, followed by hydrolysis under basic conditions *via* methyl ester **10**. Condensation of **11** with 5-amino-1-methylpyrazole produced amide **12** with a 74% yield. Inverse amide **7i** was synthesized *via* deprotection of TBS ether of **12**.

Scheme 3 illustrates the synthesis of the ester **7j**. Ester **7j** was obtained from **2** using the following steps: (1) asymmetric alkylation with alkyne **13**, (2) hydrogenation of the triple bond, (3) deprotection of TBS ethers, and (4) primary alcohol-selected condensation of 1-methylpyrazole-5-carboxylic acid.

Ketomethylene **7k** was synthesized from **2** *via* the following steps: (1) asymmetric alkylation with alkyne **17**, (2) protection of secondary alcohol, (3) reductive deprotection of Bn ester and simultaneous reduction of the triple bond, (4) condensation of 5-iodo-1-methylpyrazole *via* Weinreb amide, and (5) deprotection of bis-TBS ethers (Scheme 4).

Evaluation of growth inhibitory activity against human cancer cells

The growth inhibitory activities of analogs **7a–7k** against JFCR39,¹⁸ a panel of 39 human cancer cell lines were evaluated. The results are presented in Fig. 2. The activities of analogs **1**, **7i**,¹³ **23**, and solamin¹⁹ are shown for comparison. The *x*-axis



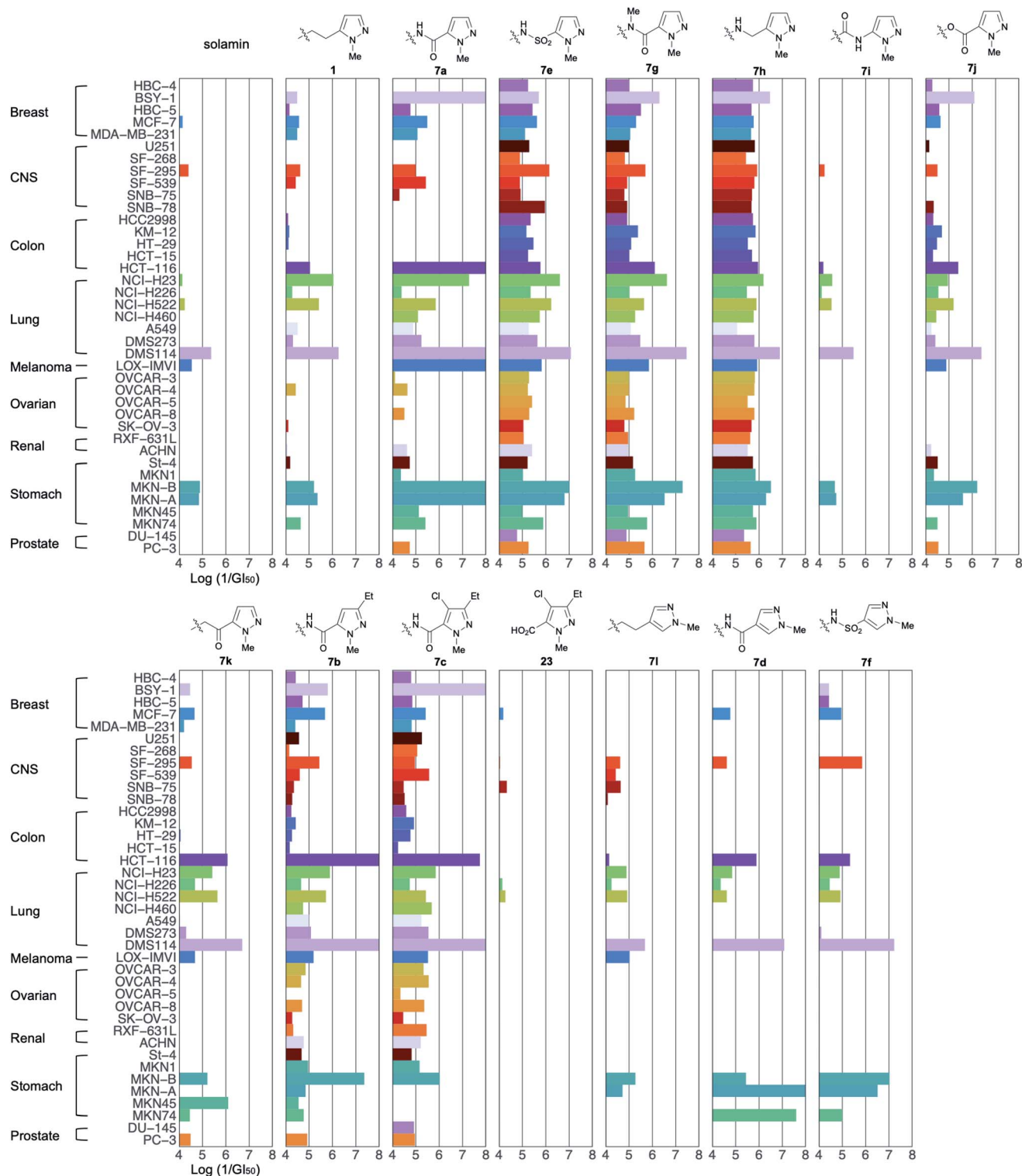


Fig. 2 Cell growth inhibition was assessed using the sulforhodamine B colorimetric assay by measuring changes in total cellular protein levels following 48 h of treatment with a given test compound. Fingerprints were obtained by calculating 50% growth inhibitory concentration (GI₅₀) values for JFCR39 cell lines. The x-axis represents the logarithm of the 1/GI₅₀ values for 39 human cancer cell lines. Absence of a bar signifies that the GI₅₀ value of the corresponding cell line is higher than 10⁻⁴ M. CNS = central nervous system.

represents the logarithm of 1/GI₅₀ (50% growth inhibitory concentration) relative to the control values for the aforementioned 39 human cancer cell lines.

First, our comparison of the activities of 1-methylpyrazole-5-yl analogs (1, 7a, 7e, and 7g–7k) revealed that the patterns could be classified into two categories: selective inhibition and broad



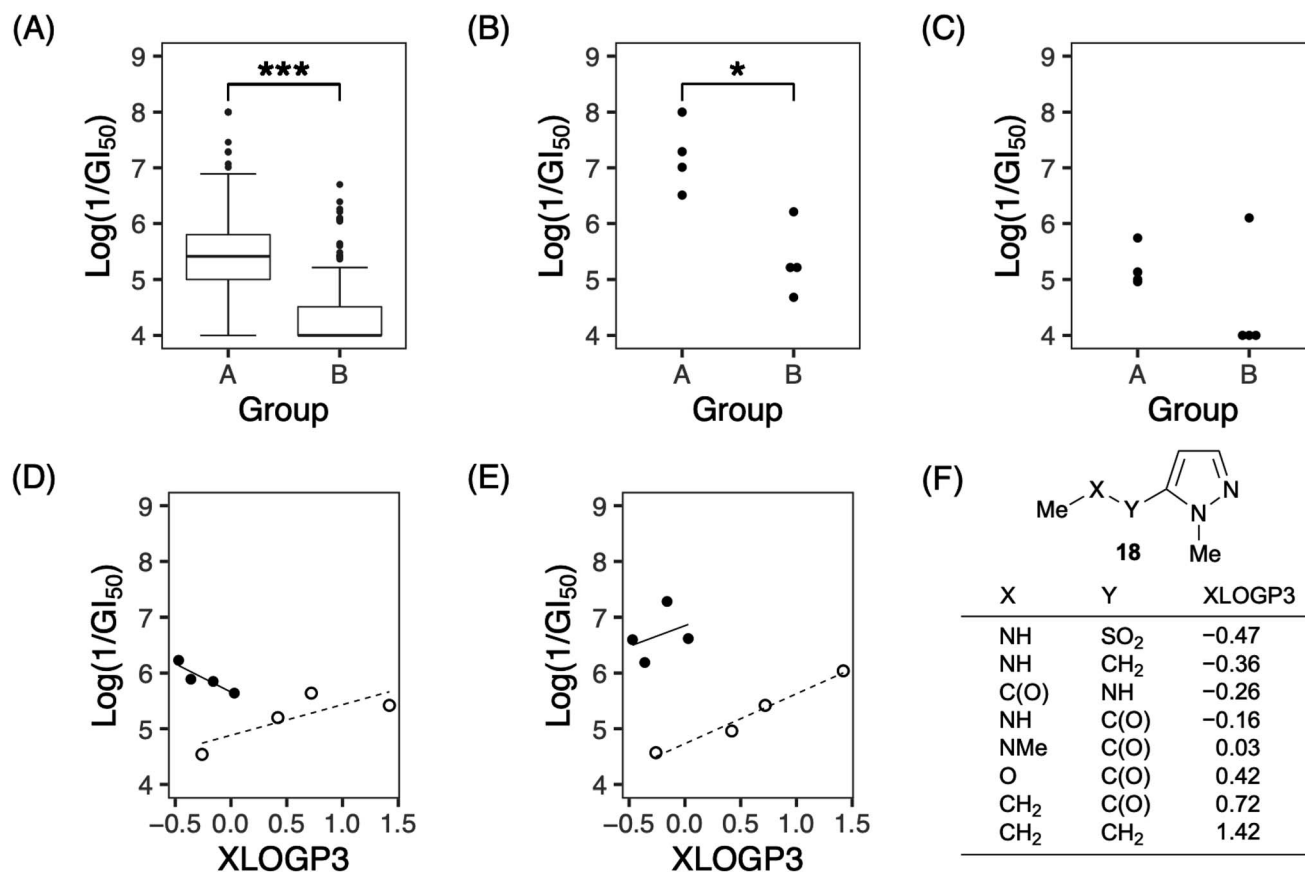


Fig. 3 Comparison of growth-inhibitory activities of analogs **1**, **7a**, **7e**, and **7g–7k**. (A) Box plot distribution of logarithm of $1/GI_{50}$ against all tested cell lines in group A (**7a**, **7e**, **7g** and **7h**) and B (**1** and **7i–7k**). Horizontal bars in the middle of each box indicate the median percentages of growth inhibition. The top and bottom of each box represent the upper and lower quartiles, respectively. The whiskers show the 5th and 95th percentiles. Data points outside the 5th and 95th percentiles are shown as dots above and below each plot. (B and C) Each plot shows distribution of logarithm of $1/GI_{50}$ against MKN-B (B) or MKN45 (C) in groups A and B. (D and E) Correlation between lipophilicity (XLOGP3) of the partial structure of analogs and logarithm of $1/GI_{50}$ against NCI-H522 (D) or NCI-H23 (E). Solid circles represent compounds of group A, and open circles represent compounds of group B. Trend lines represent the expected values predicted by the given QSAR model. (F) Partial structure of our analogs and their XLOGP3 values. *P* values were determined using the two-sided Mann–Whitney *U* test (****P* < 0.001 and **P* < 0.05).

inhibition. For instance, amide **7a** showed selective and very potent activities against some cancer cells, including BSY-1, HCT-116, NCI-H23, DMS114, LOX-IMVI, MKN-B, and MKN-A, but did not inhibit the growth of 12 types of cells in this concentration range. The selective activity was also observed for alkyl **1**, ester **7j**, and ketomethylene **7k**, although their potencies were different. Sulfonamide **7e**, 1-methylamide **7g**, and methylene amine **7h** also showed potent inhibition of DMS114, MKN-B, and MKN-A; however, their selectivities were low because they exhibited moderate activities against all other cancer cells tested. The planarity and/or hydrogen-donating properties of the amide proton attributed to the introduction of the amide bond did not affect their growth inhibitory activity; however, these properties affected their selectivities for specific cancer cell lines. Interestingly, the activity of inverse amide **7i** was deficient in contrast to that of amide **7a**.

In terms of structural features, analogs with a nitrogen atom at the 2'-position of the side chain (group A: **7a**, **7e**, **7g**, and **7h**) tended to be significantly more active than the others (group B: **1** and **7i–7k**) (Fig. 3A). These tendencies were observed against

approximately half of the cell lines (for example, MKN-B in Fig. 3B; see also Fig. S1†), while activities were not observed against the remaining cell lines (e.g., MKN45 as shown in Fig. 3C; see also Fig. S1†). When the values of lipophilicity (XLOGP3)²⁰ of the partial structure of analogs were calculated (Fig. 3F),²¹ the activities of the analogs in group A were correlated with their XLOGP3 values for most cells (Fig. S2†). For example, the relationship between the logarithm of $1/GI_{50}$ against NCI-H522 and XLOGP3 values can be expressed using linear equation (eqn (1)) (Fig. 3D). In eqn (1) and the following correlation equations, *n* refers to the number of compounds, *r* implies correlation coefficient, *s* refers to standard deviation, and the figures in parentheses indicate 95% confidence intervals. This equation allows for the design of novel analogs; analogs linked *via* boron amide might be promising since the XLOGP3 value is -0.57. In contrast, interestingly, compounds of group B showed an inverse correlation with those of group A. For example, the activities against NCI-H23 are represented by eqn (2) (Fig. 3E).



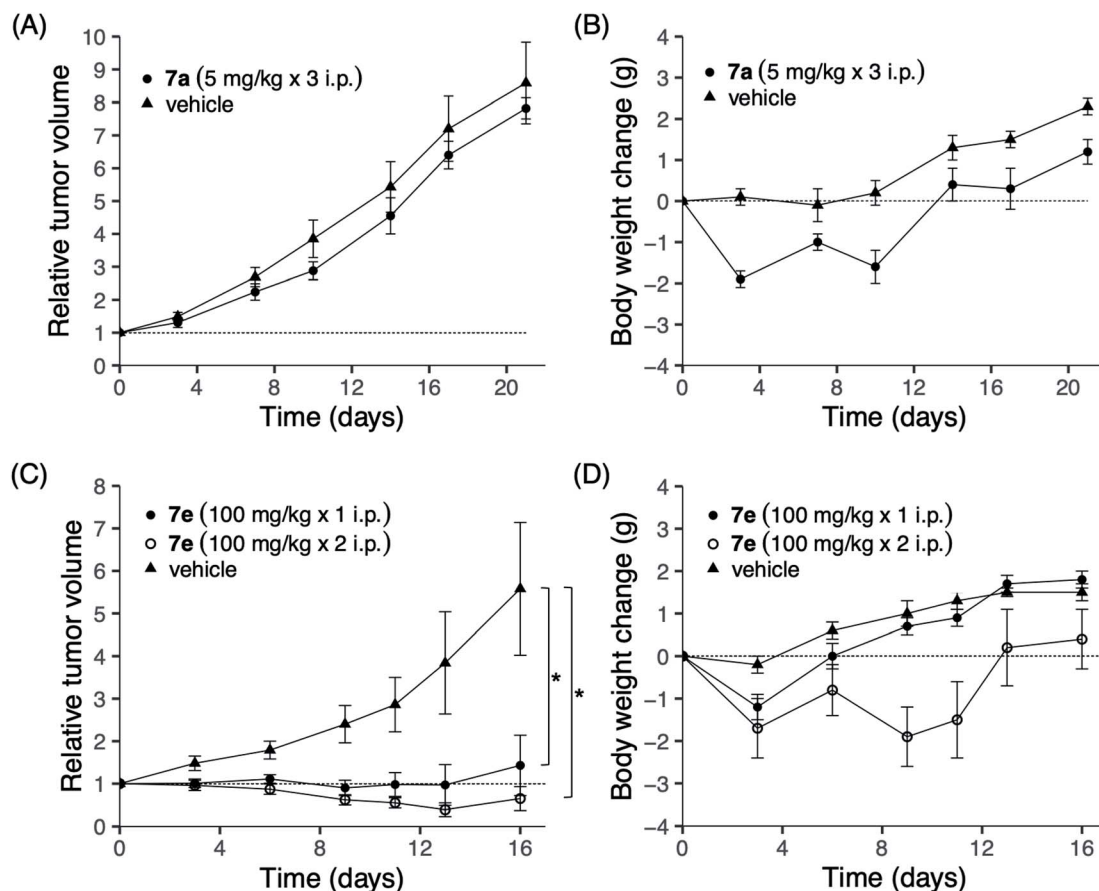


Fig. 4 Tumor growth and body weight changes in nude mice bearing a human lung cancer NCI-H23 xenograft. Nude mice were subcutaneously inoculated with a tumor fragment measuring $3 \times 3 \times 3$ mm from a subcutaneous tumor developed. When the tumor reached a volume of 100–300 mm³, the mice were divided randomly into test groups (day 0). (A and B) Amide **7a** (5 mg kg⁻¹) was intraperitoneally administered at days 0, 7 and 14. (C and D) Sulfonamide **7e** (100 mg kg⁻¹) was intraperitoneally administered on day 0, or on both days 0 and 6. Body weight and relative tumor volume are expressed as means \pm SD. * $P < 0.05$, two-sided Mann–Whitney U test compared with the vehicle-administered control group. Triangle: control group; open and closed circles: administered group.

$$\text{Log}(1/\text{GI}_{50}) = -1.016(\pm 1.326)\text{XLOGP3} + 5.659(\pm 0.407),$$

$$n = 4, r^2 = 0.845, s = 0.118 \quad (1)$$

$$\text{Log}(1/\text{GI}_{50}) = 0.896(\pm 0.438)\text{XLOGP3} + 4.732(\pm 0.365),$$

$$n = 4, r^2 = 0.975, s = 0.123 \quad (2)$$

Next, the effect of substituents in 1-methylpyrazole was evaluated (Fig. 2). Both 3-ethylpyrazole **7b** and 4-chloro-3-ethylpyrazole **7c**, with substituents identical to those of tebufenpyrad, showed selective and potent growth inhibitory activity against some cells. The selective and potent growth inhibitory activity of **7b** and **7c** was observed against the same cell lines as those observed with **7a**, except for LOX-IMVI. Therefore, the connecting groups could be more significant than the substituents of 1-methylpyrazole observed in our analogs. It is possible that carboxylic acid **23** produced by the hydrolysis of **7c** was not in its active form because of the lack of the activity, suggesting that the presence of pyrazole moiety at a certain distance from the THF moiety is vital to the activity.

Both 4-pyrazole-carboxamide **7d** and 4-pyrazole-sulfonamide **7f** showed significantly more potent activities than 4-alkyl-

pyrazole **7l**, suggesting that the connecting groups observed in our analogs might also play an essential role when present in other analogs.

The aforementioned results revealed that the growth inhibitory activities of our analogs significantly depended on the connecting group between the 1-methylpyrazole moiety and the hydrophobic alkyl chain bearing the THF ring. The importance of the nitrogen atom at the 2'-position of the side chain is unclear; however, the presence of a polar atom in this position may be essential, as 2'-hydroxy solamin, also known as murisolin, showed more potent activity than solamin.²² The positive correlation between the reduction in lipophilicity and activity suggested the presence of a water-soluble pocket at the binding site of our analogs, suggesting that more potent analogs might be discovered using synthetic analogs with less lipophilicity.

In vivo studies using mice xenografts

To clarify the efficacy of our analogs as novel anticancer agents, we conducted *in vivo* studies using mouse xenografts. Amide **7a** and sulfonamide **7e** were tested since they showed distinctive fingerprints in *in vitro* studies: while the former demonstrated



selective activity, the latter showed a broad activity. The sulfonamide **7e** was selected from the broad inhibitory analogs with similar potencies, **7e**, **7g**, and **7h**, because the total yield of **7e** (45% from **2**) was higher than those of **7g** and **7h** (which were 25% and 11%, respectively). NCI-H23 was selected for inoculation into mice because the two analogs **7a** and **7e** showed almost the same inhibition potency ($\log(1/GI_{50}$ of **7a**) = 7.28; $\log(1/GI_{50}$ of **7e**) = 6.60). The results for **7a** are shown in Fig. 4A and B. The maximum tolerated dose (MTD) of **7a** was 5 mg kg⁻¹; this finding can be attributed to its high toxicity. Three administrations of 5 mg kg⁻¹ **7a** on days 0, 7, and 14 did not show significant antitumor activity. In contrast, no death was observed after administering 100 mg kg⁻¹ of sulfonamide **7e**, which was 20-fold higher than that of **7a** (Fig. 4D). Furthermore, as shown Fig. 4C, the administration of **7e** on day 0 at a dose of 100 mg kg⁻¹ significantly inhibited tumor growth as determined on day 16 (1.43 ± 0.71 compared to tumor size at day 0), whereas the control tumor grew more than six times during this period (5.58 ± 1.56). Hence, the average tumor size in drug-treated mice compared to those in control mice was 27%. Weight loss was observed after the first administration; however, this loss was recovered later, suggesting that **7e** was well tolerated. When 100 mg kg⁻¹ of **7e** was administered twice on days 0 and 6, weight loss was observed after each administration. However, the bodyweight was eventually recovered, and a more potent tumor growth inhibition effect was observed on day 16 (12% of control). The administration of **7e** at a dose less than 100 mg kg⁻¹ can also be expected to show significant tumor growth inhibition, although this was not tested in the present study due to the lack of sufficient amounts of **7e**. This result suggests that sulfonamide **7e** is a promising novel anticancer lead, although further investigation of molecular properties, such as solubility, membrane permeability, and bioavailability, would be necessary before the analog can be used as an anticancer agent.

These results indicate that the connecting group of our analogs contributes not only to the potency of growth inhibitory activity against cancer cells but also to their safety. Sulfonamide groups are known as one of the bioisosteres of the amide bond.²³ It is not clear why the conversion of the amide bond into the sulfonamide bond in our analogs avoided the loss of bodyweight of mice; however, the metabolites, the primary amine and/or the carboxylic acid produced by hydrolysis of **7a**, might have induced the loss of bodyweight because the sulfonamide bonds are often used in place of amide to improve stability against amide bond hydrolysis by proteolytic enzymes. We previously reported that an acetogenin analog with thiophene in place of γ -lactone in solamin showed potent anti-tumor activity without acute toxicity.²⁴ Using *in vitro* data to predict *in vivo* toxicity may not be accurate; however, we might obtain an analog *via* searching with amide's bioisostere, which shows a broad spectrum activity against JFCR39 since both the sulfonamide and the thiophene carboxamide analogs show wide spectrum effects. The present SAR study is valuable because it provides another approach to demonstrate that acetogenins might lead to the development of novel anticancer agents.

Conclusions

We reported the synthesis of 11 hybrid acetogenins with various connecting groups between their pyrazole and the linker bearing the THF moiety and their growth inhibitory activities against 39 human cancer cell lines. The results demonstrated that the nitrogen atom at the 2'-position of the linker could be crucial for the inhibition of cancer growth. However, substituents in the pyrazole ring did not affect their activities. Moreover, the connecting groups divided our analogs into two categories in terms of activity: one showed selective activity and the other showed broad activity. Amide **7a**, one of the former compounds, caused substantial loss of body weight in mice and did not show significant growth inhibition against NCI-H23 in a mouse xenograft assay, although exhibited potent activity *in vitro*. In contrast, sulfonamide **7e**, one of the latter compounds, showed potent antitumor activity without acute toxicity. These data indicate the immense potential of our hybrid acetogenins as novel antitumor lead compounds. Investigation of their physical properties, bioavailability, mode of action, and structure-activity association are underway.

Experimental section

Chemistry

Melting points were measured using a Yanaco MP micro-melting point apparatus and were uncorrected. Optical rotations were measured using a JASCO DIP-360 digital polarimeter or JASCO P-1020 digital polarimeter. NMR spectra were recorded in the specified solvents using Bruker Ascend™ 500 (¹H: 500 MHz; ¹³C: 125 Hz), JEOL JNM-GX-500 (¹H: 500 MHz; ¹³C: 125 Hz), JEOL ECS-400 (¹H: 400 MHz; ¹³C: 100 Hz), JEOL JNM-AL300 (¹H: 300 MHz; ¹³C: 75 Hz), or Bruker Ultrashield™ 300 (¹H: 300 MHz; ¹³C: 75 Hz) spectrometers. Chemical shifts were recorded in ppm relative to that of the internal solvent signal [CDCl₃: 7.26 ppm (¹H NMR), 77.0 ppm (¹³C NMR)] or tetramethylsilane [0 ppm] used as the internal standard. The following abbreviations have been used: broad singlet = br s, singlet = s, doublet = d, triplet = t, quartet = q, quintet = qn, sextet = sext, septet = sep, and multiplet = m. IR absorption spectra (FT = diffuse reflectance spectroscopy) were recorded with KBr powder using a Horiba FT-210 IR spectrophotometer or as neat films on NaCl plates using a Shimadzu FTIR-8400S, and only noteworthy absorptions (in cm⁻¹) were listed. Mass spectra were obtained using a JEOL JMS-600H, JEOL JMS-700, JEOL GC-mate II, JEOL SX-102A, or JEOL LCMS-IT-TOF mass spectrometer. Column chromatography was performed using a Kanto Chemical Silica Gel 60 N (spherical, neutral, 63–210 μ m) column, and flash column chromatography was performed using a Merck Silica Gel 60 (40–63 μ m) column. All air- and moisture-sensitive reactions were carried out in flame-dried glassware in an atmosphere consisting of Ar or N₂. All solvents were dried and distilled according to standard procedures if necessary, while organic extracts were dried over anhydrous MgSO₄, filtered, and concentrated under reduced pressure using a rotary evaporator.



The synthetic procedure and characterization data for analogs **1** and **7l** are presented in the ESI.† Analogs **7a** and **7g–7j** were synthesized using procedures described in our previous report.¹⁴

N-((R)-11-[(2R,5R)-5-((1R)-1-(tert-Butyldimethylsilyloxy)tri-decyl)tetrahydrofuran-2-yl]-11-hydroxy undecyl)-1-methyl-1H-pyrazole-4-carboxamide (6d). *N,N*-Dimethylaminopyridine (3.1 mg, 0.0254 mmol) and 1-methyl-1H-pyrazole-4-carboxylic acid (5.3 mg, 0.0421 mmol) were added to a solution of **5** (16.0 mg, 0.0281 mmol) in THF (1.0 mL) with stirring at rt. 1-Ethyl-3-(3-dimethylaminopropyl)carbodiimide hydrochloride (8.1 mg, 0.0421 mmol) was added to the mixture at 0 °C and the whole mixture was stirred for 8 min at the same temperature. After stirring for 2 h at rt, water was added to the reaction mixture and the mixture was extracted with EtOAc. The combined organic layers were washed with brine prior to drying and solvent evaporation. Purification using column chromatography over silica gel with *n*-hexane/EtOAc (1 : 4) as eluent yielded **6d** (9.7 mg, 51%) as a colorless oil. $[\alpha]_D^{21} + 9.0$ (*c* 0.63 in CHCl₃); ¹H NMR (500 MHz, CDCl₃) δ : 0.06 (s, 3H), 0.08 (s, 3H), 0.87–0.90 (m, 12H), 1.26–1.66 (m, 42H), 1.91–1.94 (m, 2H), 2.45 (br s, 1H), 3.35–3.39 (m, 1H), 3.37 (dt, 2H, *J* = 7.3, 6.1 Hz), 3.53–3.57 (m, 1H), 3.77 (dt, 1H, *J* = 7.3, 6.1 Hz), 3.86 (dt, 1H, *J* = 8.5, 6.1 Hz), 3.91 (s, 3H), 5.97 (br s, 1H), 7.72 (s, 1H), 7.82 (s, 1H); ¹³C NMR (125 MHz, CDCl₃) δ : –4.6, –4.2, 14.1, 18.2, 22.6, 25.4, 25.6, 25.9 (3C), 26.9, 28.4, 28.5, 29.25, 29.30, 29.4 (2C), 29.49, 29.53, 29.55, 29.59 (2C), 29.63, 29.65, 29.73, 29.8, 31.9, 33.2, 33.4, 39.2, 39.5, 74.1, 75.2, 82.2, 82.4, 119.0, 131.6, 137.6, 162.4; IR (KBr) cm^{–1}: 3316, 1632; MS (FAB) *m/z*: 678 [M + H]⁺; HRMS (FAB) *m/z*: calcd for C₃₉H₇₆N₃O₄Si: 678.5605; found: 678.5554 [M + H]⁺.

N-((R)-11-[(2R,5R)-5-((R)-1-(tert-Butyldimethylsilyloxy)tri-decyl)tetrahydrofuran-2-yl]-11-hydroxyundecyl)-1-methyl-1H-pyrazole-5-sulfonamide (6e). 1-Methyl-1H-pyrazole-5-sulfonyl chloride **S8a** (183 mg, 1.01 mmol) and triethylamine (0.283 mL, 2.03 mmol) were added to a solution of **5** (386 mg, 0.676 mmol) in CH₂Cl₂ (10.0 mL) with stirring at rt. After stirring for 1 h, water was added to the reaction mixture and the mixture was extracted with CH₂Cl₂. The combined organic layer was dried prior to solvent evaporation. Purification using flash column chromatography over silica gel with *n*-hexane/EtOAc (7 : 1) as eluent yielded **6e** (350 mg, 73%) as a colorless oil. $[\alpha]_D^{25} + 9.0$ (*c* 0.42 in CHCl₃); ¹H NMR (500 MHz, CDCl₃) δ : 0.06 (s, 3H), 0.07 (s, 3H), 0.88 (t, 3H, *J* = 7.3 Hz), 0.89 (s, 9H), 1.21–1.52 (m, 40H), 1.60–1.68 (m, 2H), 1.91–1.95 (m, 2H), 3.04 (dt, 2H, *J* = 7.3, 6.1 Hz), 3.35–3.39 (m, 1H), 3.53–3.57 (m, 1H), 3.77 (dt, 1H, *J* = 7.3, 6.4 Hz), 3.86 (dt, 1H, *J* = 7.9, 6.1 Hz), 4.09 (s, 3H), 4.81 (t, 1H, *J* = 6.1 Hz), 6.75 (d, 1H, *J* = 2.4 Hz), 7.47 (d, 1H, *J* = 2.4 Hz); ¹³C NMR (125 MHz, CDCl₃) δ : –4.6, –4.1, 14.1, 18.3, 22.7, 25.4, 25.6, 25.9 (3C), 26.4, 28.5, 28.6, 29.0, 29.3 (2C), 29.5, 29.56, 29.59, 29.62 (4C), 29.7 (2C), 29.8, 31.9, 33.2, 33.4, 38.5, 43.3, 74.1, 75.2, 82.3, 82.4, 111.0, 137.6, 138.9; IR (KBr) cm^{–1}: 3292; MS (FAB) *m/z*: 714 [M + H]⁺; HRMS (FAB) *m/z*: calcd for C₃₈H₇₆N₃O₅SSi: 714.5275; found: 714.5262 [M + H]⁺.

N-((R)-11-[(2R,5R)-5-((R)-1-(tert-Butyldimethylsilyloxy)tri-decyl)tetrahydrofuran-2-yl]-11-hydroxyundecyl)-1-methyl-1H-pyrazole-4-sulfonamide (6f). The procedure was the same as

that used for preparation of **6e** by use of 1-methyl-1H-pyrazole-4-sulfonyl chloride **S8b** instead of 1-methyl-1H-pyrazole-5-sulfonyl chloride **S8a**, giving **6f** (yield: 73%) as a colorless oil. $[\alpha]_D^{23} + 9.6$ (*c* 0.28 in CHCl₃); ¹H NMR (500 MHz, CDCl₃) δ : 0.06 (s, 3H), 0.08 (s, 3H), 0.88 (t, 3H, *J* = 7.3 Hz), 0.89 (s, 9H), 1.26–1.51 (m, 40H), 1.56–1.68 (m, 2H), 1.88–1.97 (m, 2H), 2.95–2.99 (m, 2H), 3.34–3.41 (m, 1H), 3.55 (td, 1H, *J* = 6.1, 3.1 Hz), 3.76 (q, 1H, *J* = 6.7 Hz), 3.86 (td, 1H, *J* = 7.9, 6.1 Hz), 3.95 (s, 3H), 4.33 (br s, 1H), 7.76 (s, 1H), 7.79 (s, 1H); ¹³C NMR (125 MHz, CDCl₃) δ : –4.6, –4.2, 14.1, 18.2, 22.6, 25.4, 25.6, 25.9 (3C), 26.5, 28.4, 28.5, 29.0, 29.3, 29.35, 29.37, 29.41, 29.46, 29.53, 29.55, 29.59 (2C), 29.62 (2C), 29.8, 31.9, 33.1, 33.4, 39.5, 43.2, 74.1, 75.2, 82.2, 82.4, 122.2, 131.7, 138.5; IR (KBr) cm^{–1}: 3566, 3275; MS (FAB) *m/z*: 714 [M + H]⁺; HRMS (FAB) *m/z*: calcd for C₃₈H₇₆N₃O₅SSi: 714.5275; found: 714.5266 [M + H]⁺.

N-((11R)-11-Hydroxy-11-[(2R,5R)-5-((1R)-1-hydroxytri-decyl)tetrahydrofuran-2-yl]undecyl)-3-ethyl-1-methyl-1H-pyrazole-5-carboxamide (7b). A solution of **4** (44.3 mg, 0.0748 mmol) in THF (1.0 mL) was hydrogenated on 10% Pd–C (4.4 mg) with stirring at rt for 7 h under 3 atm pressure of hydrogen. The catalyst was filtered off through a pad of Celite® and the filtrate was concentrated under reduced pressure to give a crude **5**. *N,N*-Dimethylaminopyridine (8.9 mg, 0.0728 mmol) and 3-ethyl-1-methyl-1H-pyrazole-5-carboxylic acid **S6** (16.8 mg, 0.109 mmol) were added to a solution of the crude **5** in THF (1.5 mL) at rt. *N,N'*-Dicyclohexylcarbodiimide (22.5 mg, 0.109 mmol) was added to the mixture at 0 °C with stirring and the whole mixture was stirred for 10 min at the same temperature. After stirring for 2 h at rt, the precipitate was filtered off through a glass filter and the filtrate was concentrated under reduced pressure to give a crude **6b**. Three drops of 48% aq. HF were added to a solution of the crude **6b** in THF/MeCN (3 : 2, 1.5 mL) with stirring at rt. After stirring for 3 h at same temperature, water was added to the reaction mixture and the mixture was extracted with CH₂Cl₂. The combined organic layer was washed with brine prior to drying and solvent evaporation. Purification by flash column chromatography over silica gel with CHCl₃/MeOH (25 : 1) as eluent yielded **7b** (15.6 mg, 35% over 3 steps) as a white waxy solid. $[\alpha]_D^{25} + 8.5$ (*c* 0.55 in CHCl₃); ¹H NMR (500 MHz, CDCl₃) δ : 0.88 (t, 3H, *J* = 6.7 Hz), 1.22–1.72 (m, 42H), 1.24 (t, 3H, *J* = 7.9 Hz), 1.95–2.01 (m, 2H), 2.63 (q, 2H, *J* = 7.9 Hz), 3.35–3.42 (m, 4H), 3.80 (q, 2H, *J* = 6.7 Hz), 4.11 (s, 3H), 6.00 (br s, 1H), 6.27 (s, 1H); ¹³C NMR (75 MHz, CDCl₃) δ : 13.9, 14.1, 21.2, 22.7, 25.5 (2C), 26.9, 28.7 (2C), 29.2, 29.3, 29.4 (3C), 29.5, 29.57 (2C), 29.62 (4C), 29.7, 31.9, 33.4 (2C), 38.8, 39.5, 74.00, 74.02, 82.61, 82.64, 103.8, 135.9, 152.8, 160.1; IR (KBr) cm^{–1}: 3423, 3286, 1639; MS (FAB) *m/z*: 592 [M + H]⁺; HRMS (FAB) *m/z*: calcd for C₃₅H₆₆N₃O₄: 592.5053; found: 592.5053 [M + H]⁺.

N-((11R)-11-Hydroxy-11-[(2R,5R)-5-((1R)-1-hydroxytri-decyl)tetrahydrofuran-2-yl]undecyl)-4-chloro-3-ethyl-1-methyl-1H-pyrazole-5-carboxamide (7c). The procedure was the same as that used for preparation of **7b** by use of 4-chloro-3-ethyl-1-methyl-1H-pyrazole-5-carboxylic acid **23** instead of 3-ethyl-1-methyl-1H-pyrazole-5-carboxylic acid **S6**, giving **7c** (yield: 50% over 3 steps) as a white waxy solid. $[\alpha]_D^{24} + 9.8$ (*c* 0.75 in CHCl₃); ¹H NMR (500 MHz, CDCl₃) δ : 0.88 (t, 3H, *J* = 6.7 Hz), 1.23–1.72 (m, 42H), 1.24 (t, 3H, *J* = 7.3 Hz), 1.95–2.01 (m, 2H), 2.33 (br s,



2H), 2.64 (q, 2H, $J = 7.3$ Hz), 3.39–3.45 (m, 4H), 3.80 (q, 2H, $J = 6.7$ Hz), 4.12 (s, 3H), 6.69 (br s, 1H); ^{13}C NMR (75 MHz, CDCl_3) δ : 12.7, 14.0, 19.2, 22.6, 25.5 (2C), 26.9, 28.7 (2C), 29.2, 29.29, 29.32, 29.4 (2C), 29.48 (2C), 29.54 (2C), 29.59 (2C), 29.61, 29.7, 31.9, 33.4 (2C), 39.5, 40.4, 74.0 (2C), 82.7 (2C), 107.2, 131.4, 149.4, 158.5; IR (KBr) cm^{-1} : 3479, 3294, 1639; MS (FAB) m/z : 628 $[\text{M} + 2 + \text{H}]^+$, 626 $[\text{M} + \text{H}]^+$; HRMS (FAB) m/z : calcd for $\text{C}_{35}\text{H}_{65}\text{ClN}_3\text{O}_4$: 626.4664; found: 626.4648 $[\text{M} + \text{H}]^+$.

***N*-{[(1*R*)-11-Hydroxy-11-[(2*R*,5*R*)-5-[(1*R*)-1-hydroxy-tridecyl]-tetrahydrofuran-2-yl]undecyl]-1-methyl-1*H*-pyrazole-4-carboxamide (7d)}**. Three drops of 48% aq. HF were added to a solution of **6d** (9.0 mg, 0.0133 mmol) in THF/MeCN (2 : 1, 0.75 mL) with stirring at rt. After stirring for 2 h at the same temperature, water was added to the reaction mixture and the mixture was extracted with CH_2Cl_2 . The combined organic layer was dried prior to solvent evaporation. Purification using flash column chromatography over silica gel with EtOAc to $\text{CHCl}_3/\text{MeOH}$ (85 : 15) as eluent yielded **7d** (7.5 mg, quant.) as a white waxy solid. Mp. 92.1–93.1 °C; $[\alpha]_{\text{D}}^{25} + 11.4$ (c 0.57 in CHCl_3); ^1H NMR (500 MHz, CDCl_3) δ : 0.88 (t, 3H, $J = 7.0$ Hz), 1.26–1.71 (m, 42H), 1.97–2.02 (m, 2H), 2.36 (br s, 2H), 3.36–3.41 (m, 4H), 3.80 (dt, 2H, $J = 7.9$, 6.1 Hz), 3.92 (s, 3H), 5.73 (br s, 1H), 7.69 (s, 1H), 7.82 (s, 1H); ^{13}C NMR (75 MHz, CDCl_3) δ : 14.0, 22.6, 25.5, 25.6, 26.9, 28.7 (2C), 29.2, 29.3, 29.38 (2C), 29.44, 29.56, 29.59 (3C), 29.62 (2C), 29.63, 29.69, 29.72, 31.9, 33.5, 39.2, 39.5, 74.02, 74.03, 82.6, 82.7, 119.0, 131.7, 137.6, 162.5; IR (KBr) cm^{-1} : 3319, 1630; MS (FAB) m/z : 564 $[\text{M} + \text{H}]^+$; HRMS (FAB) m/z : calcd for $\text{C}_{33}\text{H}_{62}\text{N}_3\text{O}_4$: 564.4740; found: 564.4743 $[\text{M} + \text{H}]^+$.

***N*-{[(*R*)-11-Hydroxy-11-[(2*R*,5*R*)-5-[(*R*)-1-hydroxytridecyl]-tetrahydrofuran-2-yl]undecyl]-1-methyl-1*H*-pyrazole-5-sulfonamide (7e)}**. The procedure was the same as that used for the preparation of **7d** by use of **6e** instead of **6d**, giving **7e** (yield: 93%) as a white waxy solid. Mp. 81.5–82.5 °C; $[\alpha]_{\text{D}}^{25} + 10.4$ (c 0.57 in CHCl_3); ^1H NMR (500 MHz, CDCl_3) δ : 0.88 (t, 3H, $J = 7.0$ Hz), 1.24–1.50 (m, 40H), 1.65–1.70 (m, 2H), 1.96–2.01 (m, 2H), 2.56 (br s, 2H), 3.04 (q, 2H, $J = 6.7$ Hz), 3.41 (dt, 2H, $J = 6.1$, 4.9 Hz), 3.80 (dt, 2H, $J = 6.7$, 6.1 Hz), 4.09 (s, 3H), 4.96–4.99 (m, 1H), 6.75 (d, 1H, $J = 1.8$ Hz), 7.47 (d, 1H, $J = 1.8$ Hz); ^{13}C NMR (125 MHz, CDCl_3) δ : 14.1, 22.7, 25.5, 25.6, 26.4, 28.7 (2C), 28.9, 29.27 (2C), 29.32 (2C), 29.4, 29.55, 29.57, 29.60 (2C), 29.61, 29.63, 29.65, 29.70, 31.9, 33.4, 38.5, 43.2, 74.0, 74.1, 82.6, 82.7, 111.0, 137.6, 139.0; IR (KBr) cm^{-1} : 3445, 3277; MS (FAB) m/z : 600 $[\text{M} + \text{H}]^+$; HRMS (FAB) m/z : calcd for $\text{C}_{32}\text{H}_{62}\text{N}_3\text{O}_5\text{S}$: 600.4410; found: 600.4412 $[\text{M} + \text{H}]^+$.

***N*-{[(*R*)-11-Hydroxy-11-[(2*R*,5*R*)-5-[(*R*)-1-hydroxytridecyl]-tetrahydrofuran-2-yl]undecyl]-1-methyl-1*H*-pyrazole-4-sulfonamide (7f)}**. The procedure was the same as that used for the preparation of **7d** by use of **6f** instead of **6d**, giving **7f** (Yield: 96%) as a white waxy solid. Mp. 87.6–88.7 °C; $[\alpha]_{\text{D}}^{22} + 10.6$ (c 0.51 in CHCl_3); ^1H NMR (500 MHz, CDCl_3) δ : 0.88 (t, 3H, $J = 7.0$ Hz), 1.26–1.51 (m, 40H), 1.64–1.71 (m, 2H), 1.96–2.02 (m, 2H), 2.43 (br s, 2H, OH), 2.96 (t, 2H, $J = 7.3$ Hz), 3.41 (q, 2H, $J = 6.1$ Hz), 3.80 (td, 2H, $J = 7.3$, 6.1 Hz), 3.95 (s, 3H), 4.62 (br s, 1H), 7.76 (s, 1H), 7.81 (s, 1H); ^{13}C NMR (125 MHz, CDCl_3) δ : 14.1, 22.6, 25.5, 25.6, 26.5, 28.7 (2C), 29.0, 29.3 (3C), 29.4 (2C), 29.56 (2C), 29.59, 29.60, 29.62 (2C), 29.7 (2C), 31.9, 33.4, 39.5, 43.2, 74.00, 74.03, 82.61, 82.64, 122.2, 131.7, 138.5; IR (KBr) cm^{-1} : 3447, 3360,

3275; MS (FAB) m/z : 600 $[\text{M} + \text{H}]^+$; HRMS (FAB) m/z : calcd for $\text{C}_{32}\text{H}_{62}\text{N}_3\text{O}_5\text{S}$: 600.4410; found: 600.4410 $[\text{M} + \text{H}]^+$.

Benzyl-(13*R*)-13-[(2*R*,5*R*)-5-[(1*R*)-1-(*tert*-butyldimethylsilyloxy)tridecyl]tetrahydrofuran-2-yl]-13-hydroxytridec-11-ynoate (18). A flask was charged with $\text{Zn}(\text{OTf})_2$ (408 mg, 1.12 mmol). Vacuum (8 mmHg) was applied and the flask was heated to 120 °C for 2 h. After the flask was cooled to rt, the vacuum was released. Then, (1*R*,2*S*)-(–)-*N*-methylephedrine (215 mg, 1.20 mmol), toluene (1.5 mL), and triethylamine (0.167 mL, 1.20 mmol) were added to the flask with stirring at rt. After 2.5 h at the same temperature, a solution of **17** (320 mg, 1.12 mmol) in toluene (0.20 mL) was added to the mixture at the same temperature. After 15 min at the same temperature, **2** (331 mg, 0.801 mmol) in toluene (0.30 mL) was added to the reaction mixture and the whole mixture was stirred for 3 h at rt. The reaction was quenched with saturated NH_4Cl and the mixture was extracted with EtOAc. The combined organic layers were washed with brine prior to drying and solvent evaporation. Purification using flash column chromatography over silica gel with *n*-hexane/EtOAc (30 : 1 to 20 : 1) as eluent yielded **18** (412 mg, 73%, dr = 92 : 8) as a colorless oil. $[\alpha]_{\text{D}}^{25} + 10.0$ (c 0.61 in CHCl_3); ^1H NMR (500 MHz, CDCl_3) δ : 0.06 (s, 3H), 0.08 (s, 3H), 0.87–0.89 (m, 12H), 1.26–1.51 (m, 34H), 1.61–1.79 (m, 3H), 1.88–2.07 (m, 3H), 2.18 (td, 2H, $J = 7.3$, 2.4 Hz), 2.34 (t, 2H, $J = 7.3$ Hz), 2.35 (br s, 1H), 3.56–3.59 (m, 1H), 3.89–3.93 (m, 1H), 4.08 (td, 1H, $J = 7.3$, 3.7 Hz), 4.15–4.17 (m, 1H), 5.11 (s, 2H), 7.26–7.38 (m, 5H); ^{13}C NMR (125 MHz, CDCl_3) δ : –4.6, –4.2, 14.1, 18.2, 18.7, 22.7, 24.9, 25.5, 25.9 (3C), 27.6, 28.3, 28.5, 28.8, 29.0, 29.1, 29.2, 29.25, 29.32, 29.57 (2C), 29.60 (2C), 29.65, 29.8, 31.9, 32.9, 34.3, 65.6, 66.0, 74.9, 78.0, 82.5, 82.6, 86.3, 128.1 (3C), 128.5 (2C), 136.1, 173.6; IR (NaCl) cm^{-1} : 3503, 1740; MS (FAB) m/z : 721 $[\text{M} + \text{Na}]^+$; HRMS (FAB) m/z : calcd for $\text{C}_{43}\text{H}_{74}\text{NaO}_5\text{Si}$: 721.5203; found: 721.5222 $[\text{M} + \text{Na}]^+$.

Benzyl-(13*R*)-13-(*tert*-butyldimethylsilyloxy)-13-[(2*R*,5*R*)-5-[(1*R*)-1-(*tert*-butyldimethylsilyloxy)tridecyl]tetrahydrofuran-2-yl]tridec-11-ynoate (19). 2,6-Lutidine (0.27 mL, 2.37 mmol) was added to a solution of **18** (412 mg, 0.589 mmol) in CH_2Cl_2 (5.8 mL) with stirring at rt. TBSOTf (0.410 mL, 1.78 mmol) was added to the mixture over 15 min at same temperature. After stirring for 5 min at same temperature, water was added to the reaction mixture and the mixture was extracted with CH_2Cl_2 . The combined organic layer was dried prior to solvent evaporation. Purification by flash column chromatography over silica gel with *n*-hexane/EtOAc (50 : 1) as eluent yielded **19** (478 mg, quant.) as a colorless oil. $[\alpha]_{\text{D}}^{25} + 7.3$ (c 1.22 in CHCl_3); ^1H NMR (500 MHz, CDCl_3) δ : 0.05 (s, 3H), 0.06 (s, 3H), 0.09 (s, 3H), 0.12 (s, 3H), 0.86–0.90 (m, 21H), 1.25–1.69 (m, 37H), 1.89–1.95 (m, 3H), 2.17 (td, 2H, $J = 7.3$, 1.8 Hz), 2.35 (t, 2H, $J = 7.6$ Hz), 3.59 (dt, 1H, $J = 7.3$, 4.5 Hz), 3.97–4.02 (m, 2H), 4.37 (dt, 1H, $J = 5.5$, 1.8 Hz), 5.11 (s, 2H), 7.34–7.36 (m, 5H); ^{13}C NMR (125 MHz, CDCl_3) δ : –4.9, –4.62, –4.60, –4.2, 14.1, 18.2, 18.3, 18.7, 24.9, 25.8 (3C), 26.0 (3C), 26.9, 27.7, 28.6, 28.8, 29.06, 29.10, 29.2, 29.3 (3C), 29.6 (4C), 29.7 (2C), 29.8, 31.9, 32.5, 34.3, 66.0, 66.3, 74.5, 79.5, 82.1, 82.3, 85.5, 128.1 (3C), 128.5 (2C), 136.1, 173.7; IR (NaCl) cm^{-1} : 1740; MS (FAB) m/z : 835 $[\text{M} + \text{Na}]^+$; HRMS (FAB) m/z : calcd for $\text{C}_{49}\text{H}_{88}\text{NaO}_5\text{Si}_2$: 835.6068; found: 835.6078 $[\text{M} + \text{Na}]^+$.



(13R)-13-(tert-Butyldimethylsilyloxy)-13-((2R,5R)-5-((1R)-1-(tert-butyldimethylsilyloxy)tridecyl)tetrahydrofuran-2-yl)-tridecanoic acid (20). A solution of **19** (220 mg, 0.270 mmol) in EtOAc (2.7 mL) was hydrogenated on 10% Pd-C (22.0 mg) with stirring at rt for 7 h under 1 atm pressure of hydrogen. The catalyst was filtered off through a pad of Celite® and the filtrate was concentrated under reduced pressure. Purification by flash column chromatography over silica gel with *n*-hexane/EtOAc (10 : 1) as eluent yielded **20** (190 mg, 96%) as a colorless oil. $[\alpha]_D^{25} + 17.3$ (*c* 0.51 in CHCl₃); ¹H NMR (500 MHz, CDCl₃) δ : 0.05 (s, 6H), 0.06 (s, 6H), 0.878 (t, 3H, *J* = 7.3 Hz), 0.881 (s, 18H), 1.26–1.52 (m, 40H), 1.61–1.72 (m, 4H), 1.81–1.86 (m, 2H), 2.34 (t, 2H, *J* = 7.3 Hz), 3.56–3.60 (m, 2H), 3.91 (q, 2H, *J* = 6.1 Hz); ¹³C NMR (75 MHz, CDCl₃) δ : –4.5 (2C), –4.3 (2C), 14.1, 18.2 (2C), 22.7, 24.7, 25.9 (2C), 26.0 (6C), 27.3, 29.1, 29.2, 29.37, 29.43, 29.55, 29.63 (3C), 29.65 (3C), 29.69 (2C), 29.8 (2C), 31.9 (2C), 32.6, 34.0, 74.8 (2C), 81.8 (2C), 179.9; IR (NaCl) cm^{–1}: 1712; MS (FAB) *m/z*: 749 [M + Na]⁺; HRMS (FAB) *m/z*: calcd for C₄₂H₈₆NaO₅Si₂: 749.5911; found: 749.5895 [M + Na]⁺.

(13R)-13-(tert-Butyldimethylsilyloxy)-13-((2R,5R)-5-((1R)-1-(tert-butyldimethylsilyloxy)tridecyl)tetrahydrofuran-2-yl)-*N*-methoxy-*N*-methyltridecanamide (21). *N,N*-Dimethylamino-pyridine (1.0 mg, 0.00845 mmol), triethylamine (2.4 μ L, 0.0172 mmol), and *N,O*-dimethylhydroxylamine (2.5 mg, 0.0256 mmol) were added to a solution of **20** (12.3 mg, 0.0169 mmol) in CH₂Cl₂ (0.7 mL) with stirring at rt. 1-Ethyl-3-(3-dimethylaminopropyl) carbodiimide hydrochloride (3.9 mg, 0.0203 mmol) was added to the mixture at 0 °C and the whole mixture was stirred for 10 min at the same temperature. After stirring for 44 h at rt, water was added to the reaction mixture and the mixture was extracted with CH₂Cl₂. The combined organic layer was dried prior to solvent evaporation. Purification by flash column chromatography over silica gel with *n*-hexane/EtOAc (20 : 1 to 10 : 1) as eluent yielded **21** (12.2 mg, 94%) as a colorless oil. $[\alpha]_D^{25} + 10.9$ (*c* 0.57 in CHCl₃); ¹H NMR (400 MHz, CDCl₃) δ : 0.05 (s, 6H), 0.06 (s, 6H), 0.88 (t, 3H, *J* = 6.9 Hz), 0.88 (s, 18H), 1.25–1.72 (m, 44H), 1.78–1.86 (m, 2H), 2.41 (t, 2H, *J* = 7.3 Hz), 3.18 (s, 3H), 3.55–3.59 (m, 2H), 3.68 (s, 3H), 3.90 (q, 2H, *J* = 5.9 Hz); ¹³C NMR (75 MHz, CDCl₃) δ : –4.6 (2C), –4.3 (2C), 14.1, 18.2 (2C), 22.7, 24.6 (2C), 25.86, 25.93 (6C), 27.2, 29.3, 29.42, 29.44, 29.5, 29.60 (6C), 29.62 (4C), 29.7 (2C), 29.8, 31.9 (2C), 32.6, 61.1, 74.7 (2C), 81.7 (2C), 174.8; IR (NaCl) cm^{–1}: 1684; MS (FAB) *m/z*: 792 [M + Na]⁺; HRMS (FAB) *m/z*: calcd for C₄₄H₉₁NNaO₅Si₂: 792.6333; found: 792.6331 [M + Na]⁺.

(13R)-13-(tert-Butyldimethylsilyloxy)-13-((2R,5R)-5-((1R)-1-(tert-butyldimethylsilyloxy)tridecyl)tetrahydrofuran-2-yl)-1-(1-methyl-1H-pyrazol-5-yl)tridecan-1-one (22). *n*-BuLi (1.65 M in *n*-hexane, 0.10 mL, 0.165 mmol) was added over 10 min to a solution of 5-iodo-1-methyl-1H-pyrazole (34.7 mg, 0.167 mmol) in THF (0.40 mL) with stirring at –30 °C. After stirring for 30 min at same temperature, **21** (42.7 mg, 0.0554 mmol) in THF (0.15 mL) was added to the reaction mixture at same temperature. After stirring for 5 min at same temperature, saturated NH₄Cl was added to the reaction mixture and the mixture was extracted with EtOAc. The combined organic layer was washed with brine prior to drying and solvent evaporation.

Purification by flash column chromatography over silica gel with *n*-hexane/EtOAc (30 : 1 to EtOAc) as eluent yielded **22** (19.3 mg, 44%, brsm 66%) as a colorless oil. $[\alpha]_D^{25} + 24.6$ (*c* 0.32 in CHCl₃); ¹H NMR (400 MHz, CDCl₃) δ : 0.05 (s, 6H), 0.06 (s, 6H), 0.86–0.89 (m, 21H), 1.22–1.56 (m, 40H), 1.65–1.72 (m, 4H), 1.80–1.84 (m, 2H), 2.83 (t, 2H, *J* = 7.3 Hz), 3.58 (dt, 2H, *J* = 6.8, 4.6 Hz), 3.85–3.94 (m, 2H), 4.17 (s, 3H), 6.82 (d, 1H, *J* = 2.3 Hz), 7.46 (d, 1H, *J* = 2.3 Hz); ¹³C NMR (75 MHz, CDCl₃) δ : –4.5 (2C), –4.3 (2C), 14.1, 18.2 (2C), 22.7, 24.3, 25.9, 26.0 (6C), 27.3, 29.3, 29.36, 29.44, 29.5, 29.60 (2C), 29.62 (3C), 29.63 (3C), 29.65 (2C), 29.68, 29.8 (2C), 31.9, 32.6, 40.2, 40.6, 74.8 (2C), 81.8 (2C), 111.2, 137.5, 138.5, 192.0; IR (NaCl) cm^{–1}: 1676; MS (FAB) *m/z*: 813 [M + Na]⁺; HRMS (FAB) *m/z*: calcd for C₄₆H₉₀N₂NaO₄Si₂: 813.6337; found: 813.6335 [M + Na]⁺.

(13R)-13-Hydroxy-13-((2R,5R)-5-((1R)-1-hydroxytridecyl)tetrahydrofuran-2-yl)-1-(1-methyl-1H-pyrazol-5-yl)tridecan-1-one (7k). The procedure was the same as that used for the preparation of **7d** using **22** instead of **6d**, giving **7k** (yield: quant.) as a white waxy solid. Mp. 62.5–63.2 °C; $[\alpha]_D^{23} + 7.9$ (*c* 0.33 in CHCl₃); ¹H NMR (500 MHz, CDCl₃) δ : 0.88 (t, 3H, *J* = 6.9 Hz), 1.26–1.73 (m, 44H), 1.93–2.03 (m, 2H), 2.36 (br s, 2H), 2.83 (t, 2H, *J* = 7.3 Hz), 3.40 (q, 2H, *J* = 5.9 Hz), 3.78–3.83 (m, 2H), 4.17 (s, 3H), 6.82 (d, 1H, *J* = 2.3 Hz), 7.46 (d, 1H, *J* = 2.3 Hz); ¹³C NMR (125 MHz, CDCl₃) δ : 14.1, 22.7, 24.3, 25.6 (2C), 28.7 (2C), 29.2, 29.3, 29.40, 29.43, 29.56 (3C), 29.58, 29.61 (2C), 29.63, 29.65, 29.66, 29.70, 31.9, 33.5 (2C), 40.2, 40.6, 74.0 (2C), 82.62, 82.63, 111.2, 137.5, 138.5, 192.0; IR (NaCl) cm^{–1}: 3447, 1738; MS (FAB) *m/z*: 563 [M + H]⁺; HRMS (FAB) *m/z*: calcd for C₃₄H₆₃N₂O₄: 563.4788; found: 563.4810 [M + H]⁺.

Biology

Determination of cell growth inhibition profiles (fingerprint). This study was carried out at the Cancer Chemotherapy Center of the Japanese Foundation for Cancer Research. The screening panel consisted of the following 39 human cancer cell lines (JFCR39): breast cancer HBC-4, BSY-1, HBC-5, MCF-7, and MDA-MB-231; brain cancer U251, SF-268, SF-295, SF-539, SNB-75, and SNB-78; colon cancer HCC2998, KM-12, HT-29, HCT-15, and HCT-116; lung cancer NCI-H23, NCI-H226, NCI-H522, NCI-H460, A549, DMS273, and DMS114; melanoma LOX-IMVI; ovarian cancer OVCAR-3, OVCAR-4, OVCAR-5, OVCAR-8, and SK-OV-3; renal cancer RXF-631L and ACHN; stomach cancer St-4, MKN1, MKN-B, MKN-A, MKN45, and MKN74; prostate cancer DU-145 and PC-3. Inhibition of cell growth was assessed by measuring changes in total cellular protein levels after 48 h of treatment with a given test compound using the sulforhodamine B colorimetric assay. The molar concentration of the test compound required for 50% growth inhibitory concentration (GI₅₀) of the cells was calculated as previously reported. The detailed method has been described previously.¹⁸

Antitumor activity evaluation. Animal care and treatment were performed in accordance with the guidelines of the Animal Use and Care Committee of the Japanese Foundation for Cancer Research and experiments were approved by the Animal Use and Care Committee of the Japanese Foundation for Cancer Research. The procedures conformed to the NIH Guide for the



Care and Use of Laboratory Animals. Female nude mice with BALB/c genetic background were purchased from Charles River Japan (Yokohama, Japan). Mice were maintained under specific pathogen-free conditions and provided *ad libitum* access to sterile food and water. Human tumor xenografts were developed by subcutaneously inoculating nude mice with $3 \times 3 \times 3$ mm tumor fragments of human cancer cells. The drug was dissolved in dimethyl sulfoxide (DMSO; Sigma-Aldrich) to obtain a stock concentration of 100 mg mL^{-1} . Before administration, the stock solution was mixed with an equal volume of Cremophor EL (Sigma) and finally diluted with saline to yield a concentration of 10 mg mL^{-1} in 10% DMSO/10% Cremophor EL/80% saline. When the tumors reached $100\text{--}300 \text{ mm}^3$ in size, the drug was intraperitoneally administered thrice on days 0, 7, and 14 (amide **7a**, 5 mg kg^{-1}), once on day 0 (sulfonamide **7e**, 100 mg kg^{-1}), and twice on days 0 and 6. The length (*L*) and width (*W*) of the subcutaneous tumor mass were measured using calipers in live mice, and tumor volume (TV) was calculated using the following equation: $\text{TV} = (L \times W^2)/2$. T/C (%) was calculated as follows: $\text{TV with drug}/\text{TV control} \times 100$. To assess toxicity, we measured the body weights of the tumor-bearing mice.

Statistical analysis

All statistical analyses were performed using Rstudio 2021.09.1 + 372 for Mac,²⁵ which is a graphical user interface for R version 4.1.2 (2021-11-01).²⁶ The differences were considered significant when $*P < 0.05$, $**P < 0.01$, or $***P < 0.001$.

Author contributions

S. D., and N. K. participated in the research design. K. O., T. F., M. O., S. D., and N. K. conducted the experiments. K. O., M. O., S. D., and N. K. performed the data analysis. K. O., M. O., A. A., S. D., H. I., M. Y., and N. K. wrote or contributed to the writing of the manuscript.

Conflicts of interest

There are no conflicts to declare.

Acknowledgements

The *in vitro* antiproliferative activities of acetogenin analogs against human cancer cell lines were examined by the Screening Committee of Anticancer Drugs supported by a Grant-in-Aid for Scientific Research on Innovative Areas, Scientific Support Programs for Cancer Research, from the Ministry of Education, Culture, Sports, Science and Technology, Japan (MEXT). We thank Mr Takahiro Tatsukawa for his technical assistance in the preliminary part of this study and Prof. Tetsuaki Tanaka and Prof. Takehiko Yoshimitsu for their helpful discussions. This study was supported in part by JSPS KAKENHI [grant numbers 25460159, 16K08330 (N. K.), 16H05105 (S. D. and A. A.)], the MEXT-Supported Program for the Strategic Research Foundation at Private Universities, 2015–2019 [Grant Number

S1511024L] (N. K.), a Kyoto Pharmaceutical University Fund for the Promotion of Scientific Research (N. K.), and a research grant from the Nippon Foundation (S. D.).

Notes and references

- 1 Cancer Today, <https://geo.iarc.fr/today>, (accessed January 2022).
- 2 For recent review of mitochondrial complex inhibitors for cancer therapy, see: M. Bedi, M. Ray and A. Ghosh, *Mol. Cell. Biochem.*, 2022, **477**, 345–361.
- 3 J. Yoshida, T. Ohishi, H. Abe, S. Ohba, H. Inoue, I. Usami, M. Amemiya, R. Oriez, C. Sakashita, S. Dan, M. Sugawara, T. Kawaguchi, J. Ueno, Y. Asano, A. Ikeda, M. Takamatsu, G. Amori, Y. Kondoh, K. Honda, H. Osada, T. Noda, T. Watanabe, T. Shimizu, M. Shibasaki and M. Kawada, *iScience*, 2022, **24**, 103497.
- 4 Solasia Pharma K. K., <https://solasia.co.jp/en/pipeline/sp02.html>, (accessed January 2022).
- 5 (a) N. Kojima, H. Hayashi, H. Iwasaki and M. Yamashita, *Chem. Pharm. Bull.*, 2020, **68**, 675–678; (b) N. Kojima, M. Abe, Y. Suga, K. Ohtsuki, T. Tanaka, H. Iwasaki, M. Yamashita and H. Miyoshi, *Bioorg. Med. Chem. Lett.*, 2013, **23**, 1217–1219; (c) N. Kojima, Y. Suga, H. Hayashi, T. Yamori, T. Yoshimitsu and T. Tanaka, *Bioorg. Med. Chem. Lett.*, 2011, **21**, 5745–5749; (d) N. Kojima, H. Hayashi, S. Suzuki, H. Tominaga, N. Maezaki, T. Tanaka and T. Yamori, *Bioorg. Med. Chem. Lett.*, 2008, **18**, 6451–6453; (e) N. Maezaki, N. Kojima and T. Tanaka, *Synlett*, 2006, **7**, 993–1003; (f) N. Kojima, *Yakugaku Zasshi*, 2004, **124**, 673–681.
- 6 For recent review of isolation and biological activity of annonaceous acetogenins, see: A. Neske, J. R. Hidalgo, N. Cabedo and D. Cortes, *Phytochemistry*, 2020, **174**, 112332.
- 7 For recent review of medicinal chemistry of annonaceous acetogenins, see: N. Kojima and T. Tanaka, *Molecules*, 2009, **14**, 3621–3661.
- 8 M. Murai and H. Miyoshi, *Biochim. Biophys. Acta, Bioenerg.*, 2016, **1857**, 884–891.
- 9 Heterocyclic acetogenin analogs in place of γ -lactone by other groups, see: (a) E. R. Gould, E. F. B. King, S. K. Menzies, A. L. Fraser, L. B. Tulloch, M. K. Zacharova, T. K. Smith and G. J. Florence, *Bioorg. Med. Chem.*, 2017, **25**, 6126–6136; (b) Y. Liu, Q. Xiao, Y. Liu, Z. Li, Y. Qiu, G.-B. Zhou, Z.-J. Yao and S. Jiang, *Eur. J. Med. Chem.*, 2014, **78**, 248–258; (c) Y.-J. Chen, S. Jin, J. Xi and Z.-J. Yao, *Tetrahedron*, 2014, **70**, 4921–4928; (d) R. A. Duval, G. Lewin, E. Peris, N. Chahboune, A. Garofano, S. Dröse, D. Cortes, U. Brandt and R. Hocquemiller, *Biochemistry*, 2006, **45**, 2721–2728; (e) R. A. Duval, E. Poupon, V. Romero, E. Peris, G. Lewin, D. Cortes, U. Brandt and R. Hocquemiller, *Tetrahedron*, 2006, **62**, 6248–6257; (f) R. Duval, G. Lewin and R. Hocquemiller, *Bioorg. Med. Chem.*, 2003, **11**, 3439–3446.
- 10 I. Y. Shiraishi, M. Murai, N. Sakiyama, K. Ifuku and H. Miyoshi, *Biochemistry*, 2012, **51**, 1953–1963.



- 11 (a) Y. Nakanishi, F.-R. Chang, C.-C. Liaw, Y.-C. Wu, K. F. Bastow and K.-H. Lee, *J. Med. Chem.*, 2003, **46**, 3185–3188; (b) S. C. Sinha and E. Keinan, *J. Am. Chem. Soc.*, 1993, **115**, 4891–4892; (c) S. H. Myint, D. Cortes, A. Laurens, R. Hocquemiller, M. Lebeuf, A. Cavé, J. Cotte and A.-M. Quéro, *Phytochemistry*, 1991, **30**, 3335–3338.
- 12 For reviews of hybridization as an approach to new drug, see: (a) H. M. S. Kumar, L. Herrmann and S. B. Tsogoeva, *Bioorg. Med. Chem. Lett.*, 2020, **30**, 127514; (b) G. Bérubé, *Expert Opin. Drug Discovery*, 2016, **11**, 281–305; (c) K. Nepali, S. Sharma, M. Sharma, P. M. S. Bedi and K. L. Dhar, *Eur. J. Med. Chem.*, 2014, **77**, 422–487.
- 13 N. Kojima, T. Fushimi, N. Maezaki, T. Tanaka and T. Yamori, *Bioorg. Med. Chem. Lett.*, 2008, **18**, 1637–1641.
- 14 N. Kojima, T. Fushimi, T. Tatsukawa, T. Yoshimitsu, T. Tanaka, T. Yamori, S. Dan, H. Iwasaki and M. Yamashita, *Eur. J. Med. Chem.*, 2013, **63**, 833–839.
- 15 (a) N. Kojima, N. Maezaki, H. Tominaga, M. Yanai, D. Urabe and T. Tanaka, *Chem.-Eur. J.*, 2004, **10**, 672–680; (b) N. Kojima, N. Maezaki, H. Tominaga, M. Asai, M. Yanai and T. Tanaka, *Chem.-Eur. J.*, 2003, **9**, 5428; (c) N. Maezaki, N. Kojima, H. Tominaga, M. Yanai and T. Tanaka, *Org. Lett.*, 2003, **5**, 1411–1414; (d) N. Maezaki, N. Kojima, M. Asai, H. Tominaga and T. Tanaka, *Org. Lett.*, 2002, **4**, 2977–2980.
- 16 D. E. Frantz, R. Fässler and E. M. Carreira, *J. Am. Chem. Soc.*, 2000, **122**, 1806–1807.
- 17 T. Matsumoto, N. Kojima, A. Akatsuka, T. Yamori, S. Dan, H. Iwasaki and M. Yamashita, *Tetrahedron*, 2017, **73**, 2359–2366.
- 18 (a) S. Dan, M. Okamura, M. Seki, K. Yamazaki, H. Sugita, M. Okui, Y. Mukai, H. Nishimura, R. Asaka, K. Nomura, Y. Ishikawa and T. Yamori, *Cancer Res.*, 2010, **70**, 4982–4994; (b) S. Yaguchi, Y. Fukui, I. Koshimizu, H. Yoshimi, T. Matsuno, H. Gouda, S. Hirono, K. Yamazaki and T. Yamori, *J. Natl. Cancer Inst.*, 2006, **98**, 545–556; (c) T. Yamori, A. Matsunaga, S. Sato, K. Yamazaki, A. Komi, K. Ishizu, I. Mita, H. Edatsugi, Y. Matsuba, K. Takezawa, O. Nakanishi, H. Kohno, Y. Nakajima, H. Komatsu, T. Andoh and T. Tsuruo, *Cancer Res.*, 1999, **59**, 4042–4049.
- 19 N. Kojima, T. Morioka, D. Urabe, M. Yano, Y. Suga, N. Maezaki, A. Ohashi-Kobayashi, Y. Fujimoto, M. Maeda, T. Yamori, T. Yoshimitsu and T. Tanaka, *Bioorg. Med. Chem.*, 2010, **18**, 8630–8641.
- 20 T. Cheng, Y. Zhao, X. Li, F. Lin, Y. Xu, X. Zhang, Y. Li, R. Wang and L. Lai, *J. Chem. Inf. Model.*, 2007, **47**, 2140–2148.
- 21 A. Daina, O. Michielin and V. Zoete, XLOGP3 values of compounds were calculated using the SwissADME online tool, *Sci. Rep.*, 2017, **7**, 42717, (<https://www.swissadme.ch>).
- 22 N. Maezaki, H. Tominaga, N. Kojima, M. Yanai, D. Urabe, R. Ueki, T. Tanaka and T. Yamori, *Chem.-Eur. J.*, 2005, **11**, 6237–6245.
- 23 S. Kumari, A. V. Carmona, A. K. Tiwari and P. C. Trippier, *J. Med. Chem.*, 2020, **63**, 12290–12358.
- 24 (a) S. Ando, C. Moyama, N. Kojima, M. Fujita, K. Ohta, Y. Kohno, H. Ii and S. Nakata, *Biochem. Biophys. Res. Commun.*, 2022, **591**, 62–67; (b) K. Ohta, A. Akatsuka, S. Dan, H. Iwasaki, M. Yamashita and N. Kojima, *Chem. Pharm. Bull.*, 2021, **69**, 1029–1033; (c) T. Matsumoto, A. Akatsuka, S. Dan, H. Iwasaki, M. Yamashita and N. Kojima, *Tetrahedron*, 2020, **76**, 131058; (d) A. Akatsuka, N. Kojima, M. Okamura, S. Dan and T. Yamori, *Pharmacol. Res. Perspect.*, 2016, **4**, e00246; (e) N. Kojima, Y. Suga, T. Matsumoto, T. Tanaka, A. Akatsuka, T. Yamori, S. Dan, H. Iwasaki and M. Yamashita, *Bioorg. Med. Chem.*, 2015, **23**, 1276–1283; (f) N. Kojima, T. Fushimi, T. Tatsukawa, T. Tanaka, M. Okamura, A. Akatsuka, T. Yamori, S. Dan, H. Iwasaki and M. Yamashita, *Eur. J. Med. Chem.*, 2014, **86**, 684–689.
- 25 R Core Team, *R: A Language and Environment for Statistical Computing*, R Foundation for Statistical Computing, Vienna, Austria, 2021.
- 26 RStudio Team, *RStudio: Integrated Development Environment for R*, RStudio, PBC, Boston, MA, 2021.

